



Towards Unsupervised Deep Graph Structure Learning

Yixin Liu¹, Yu Zheng², Daokun Zhang^{1,3}, Hongxu Chen⁴, Hao Peng⁵, Shirui Pan^{1*}

¹Monash University ²La Trobe University ³Monash Suzhou Research Institute

⁴University of Technology Sydney ⁵Beihang University

{yixin.liu, daokun.zhang, shirui.pan}@monash.edu;

yu.zheng@latrobe.edu.au; hongxu.chen@uts.edu.au; penghao@buaa.edu.cn

Code : <https://github.com/GRAND-Lab/SUBLIME>

WWW_2022



gesis
Leibniz-Institut
für Sozialwissenschaften



Reported by Xinsheng Wang



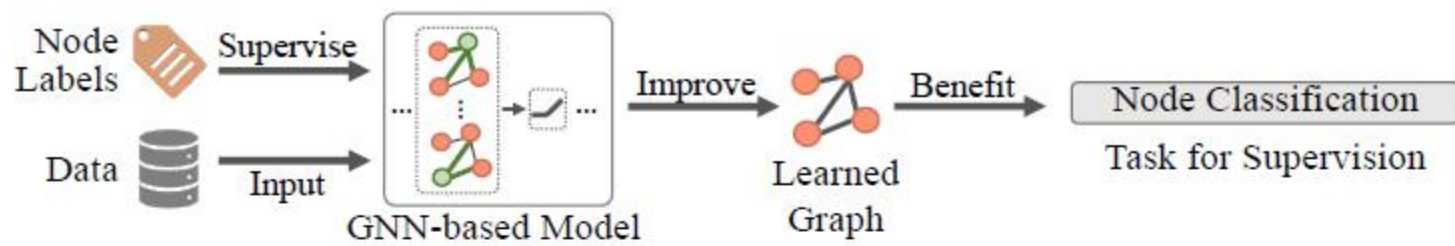
1. Introduction

2. Method

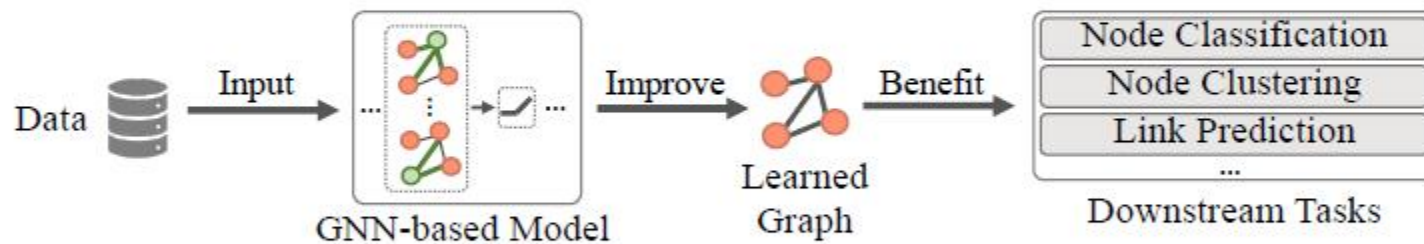
3. Experiments



Introduction



(a) Supervised GSL paradigm.



(b) Our proposed unsupervised GSL paradigm.

Figure 1: Concept maps of (a) the existing supervised GSL paradigm and (b) our proposed unsupervised GSL paradigm.

Method

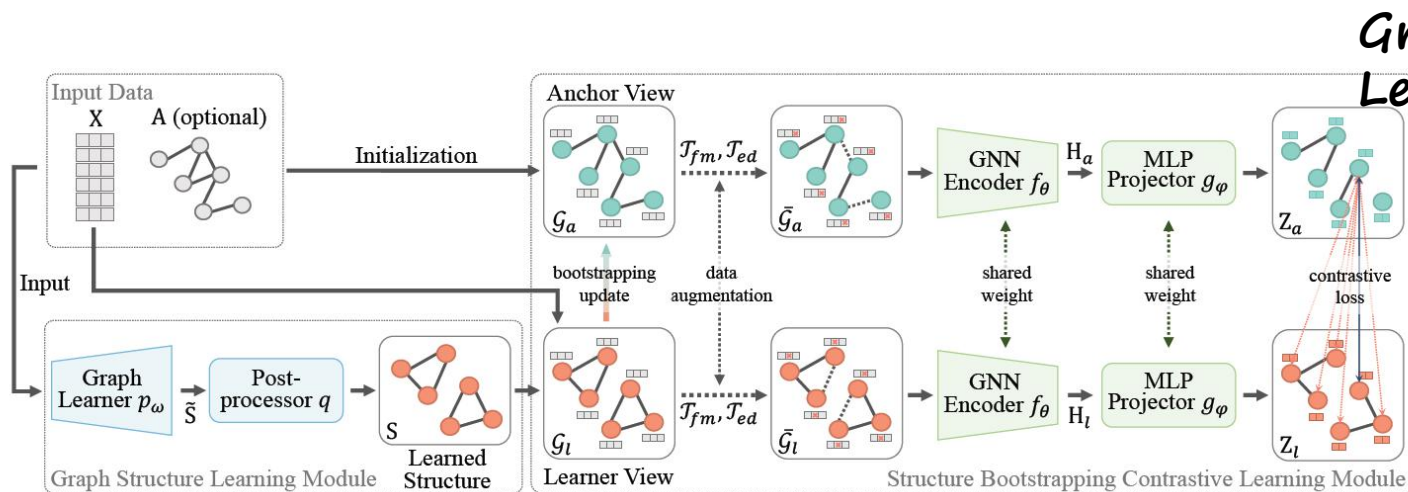


Figure 2: The overall pipeline of SUBLIME. In the graph structure learning module, the graph learner p_ω generates the sketched adjacency matrix \tilde{S} , and then the post processor q converts \tilde{S} into the learned structure S . After that, the structure bootstrapping contrastive learning module optimizes S by maximizing the agreement between the learner view and anchor view.

Graph
Learner

Full Graph
Parameterization, FGP

$$\tilde{S} = p_\omega^{FGP} = \sigma(\Omega), \quad (1)$$

where $\omega = \Omega \in \mathbb{R}^{n \times n}$ is a parameter matrix

$$\tilde{S} = p_\omega^{ML}(X, A) = \phi(h_\omega(X, A)) = \phi(E), \quad (2)$$

Attentive

Learner

$$E^{(l)} = h_w^{(l)}(E^{(l-1)}) = \sigma([e_1^{(l-1)} \odot \omega^{(l)}, \dots, e_n^{(l-1)} \odot \omega^{(l)}]^\top), \quad (3)$$

MLP Learner

$$E^{(l)} = h_w^{(l)}(E^{(l-1)}) = \sigma(E^{(l-1)}\Omega^{(l)}), \quad (4)$$

GNN

$$E^{(l)} = h_w^{(l)}(E^{(l-1)}, A) = \sigma(\tilde{D}^{-\frac{1}{2}}\tilde{A}\tilde{D}^{-\frac{1}{2}}E^{(l-1)}\Omega^{(l)}), \quad (5)$$

Method

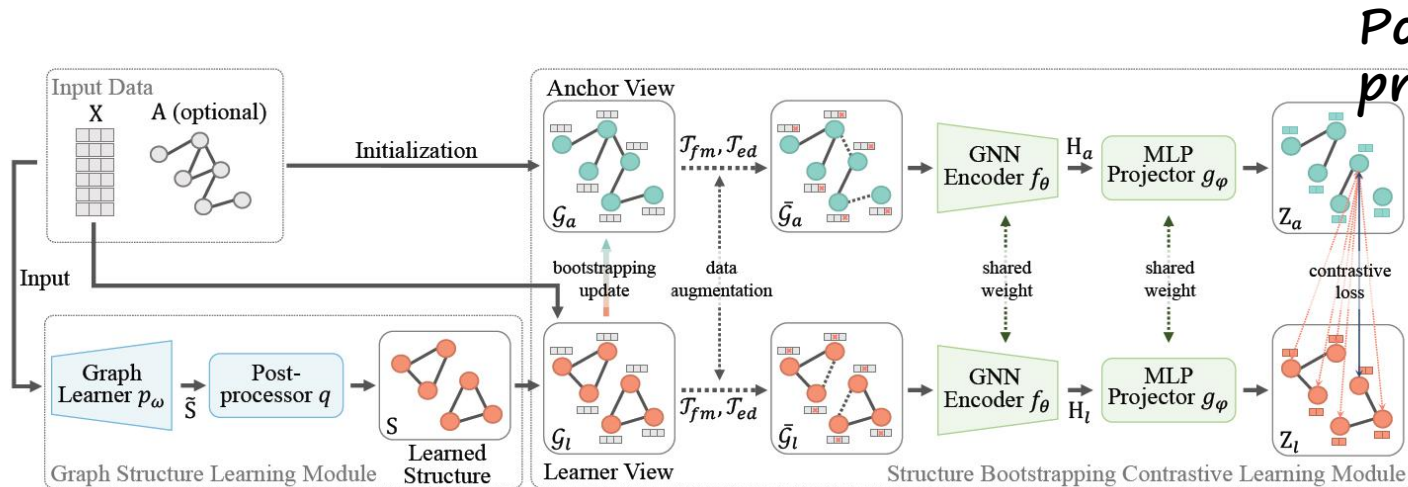


Figure 2: The overall pipeline of SUBLIME. In the graph structure learning module, the graph learner p_ω generates the sketched adjacency matrix \tilde{S} , and then the post processor q converts \tilde{S} into the learned structure S . After that, the structure bootstrapping contrastive learning module optimizes S by maximizing the agreement between the learner view and anchor view.

Post-processor
Sparsification

$$\tilde{S}_{ij}^{(sp)} = q_{sp}(\tilde{S}_{ij}) = \begin{cases} \tilde{S}_{ij}, & \tilde{S}_{ij} \in \text{top-k}(\tilde{S}_i), \\ 0, & \tilde{S}_{ij} \notin \text{top-k}(\tilde{S}_i), \end{cases} \quad (6)$$

Symmetrization and

$$\tilde{S}^{(sym)} = q_{sym}(q_{act}(\tilde{S}^{(sp)})) = \frac{\sigma_q(\tilde{S}^{(sp)}) + \sigma_q(\tilde{S}^{(sp)})^T}{2}, \quad (7)$$

define $\sigma_q(\cdot)$ as ReLU function

Normalization

$$S = q_{norm}(\tilde{S}^{(sym)}) = (\tilde{D}^{(sym)})^{-\frac{1}{2}} \tilde{S}^{(sym)} (\tilde{D}^{(sym)})^{-\frac{1}{2}}, \quad (8)$$

Method

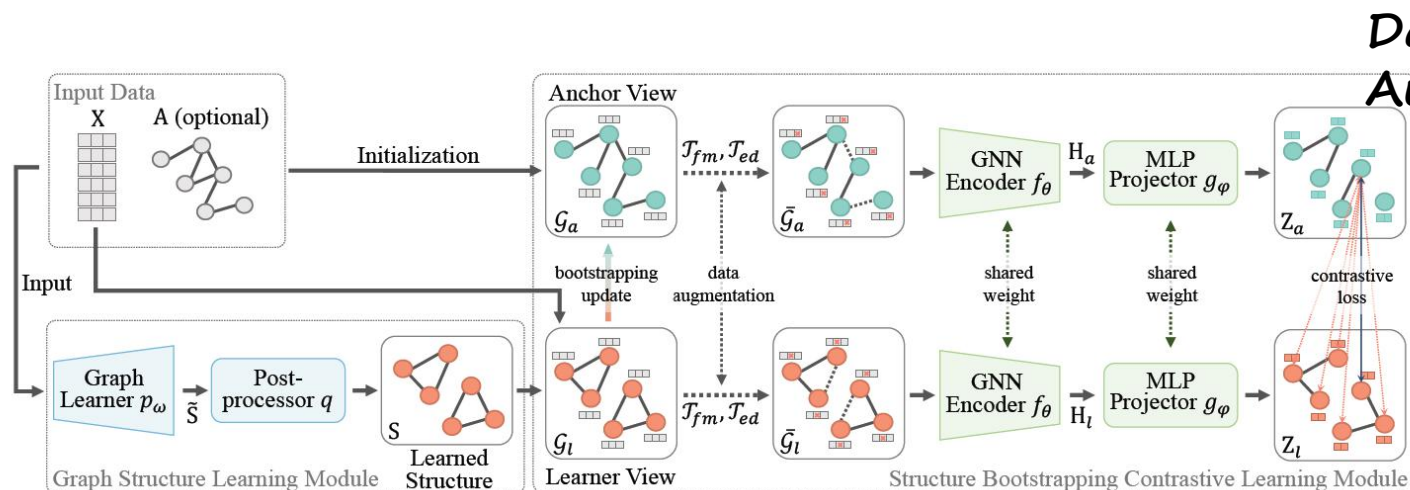


Figure 2: The overall pipeline of SUBLIME. In the graph structure learning module, the graph learner p_ω generates the sketched adjacency matrix \hat{S} , and then the post processor q converts \hat{S} into the learned structure S . After that, the structure bootstrapping contrastive learning module optimizes S by maximizing the agreement between the learner view and anchor view.

Data Augmentation

$$\bar{X} = \mathcal{T}_{fm}(X) = [x_1 \odot m^{(x)}, \dots, x_n \odot m^{(x)}]^\top, \quad (9)$$

Edge

$$\bar{A} = \mathcal{T}_{ed}(A) = A \odot M^{(a)}, \quad (10)$$

$$\bar{G}_l = (\mathcal{T}_{ed}(S), \mathcal{T}_{fm}(X)), \quad \bar{G}_a = (\mathcal{T}_{ed}(A_a), \mathcal{T}_{fm}(X)), \quad (11)$$

Method

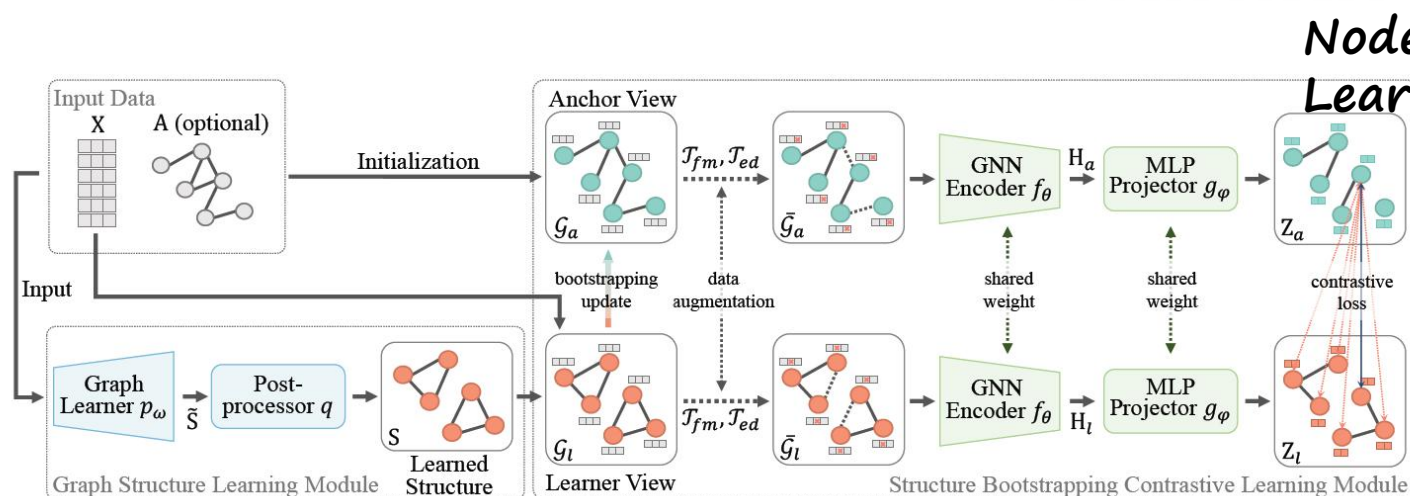


Figure 2: The overall pipeline of SUBLIME. In the graph structure learning module, the graph learner p_ω generates the sketched adjacency matrix \hat{S} , and then the post processor q converts \hat{S} into the learned structure S . After that, the structure bootstrapping contrastive learning module optimizes S by maximizing the agreement between the learner view and anchor view.

Node-level Contrastive Learning

GNN-based

$$H_l = f_\theta(\bar{G}_l), H_a = f_\theta(\bar{G}_a), \quad (12)$$

MLP-based

$$Z_l = g_\phi(H_l), Z_a = g_\phi(H_a), \quad (13)$$

Node-level contrastive loss

$$\mathcal{L} = \frac{1}{2n} \sum_{i=1}^n [\ell(z_{l,i}, z_{a,i}) + \ell(z_{a,i}, z_{l,i})], \quad (14)$$

$$\ell(z_{l,i}, z_{a,i}) = \log \frac{e^{\text{sim}(z_{l,i}, z_{a,i})/t}}{\sum_{k=1}^n e^{\text{sim}(z_{l,i}, z_{a,k})/t}},$$

$\text{sim}(\cdot, \cdot)$ is the cosine similarity function

Structure Bootstrapping Mechanism

$$A_a \leftarrow \tau A_a + (1 - \tau) S. \quad (15)$$

Experiments

Table 1: Node classification accuracy (percentage with standard deviation) in structure inference scenario. Available data for *graph structure learning* during the training phase is shown in the first column, where X, Y, A_{knn} correspond to node features, labels and the adjacency matrix of kNN graph, respectively. The highest and second highest results are highlighted with **boldface** and underline, respectively. The symbol “OOM” means out of memory.

Available Data for GSL	Method	Dataset							
		Cora	Citeseer	Pubmed	ogbn-arxiv	Wine	Cancer	Digits	20news
-	LR	60.8±0.0	62.2±0.0	72.4±0.0	52.5±0.0	92.1±1.3	93.3±0.5	85.5±1.5	42.7±1.7
-	Linear SVM	58.9±0.0	58.3±0.0	72.7±0.1	51.8±0.0	93.9±1.6	90.6±4.5	87.1±1.8	40.3±1.4
-	MLP	56.1±1.6	56.7±1.7	71.4±0.0	54.7±0.1	89.7±1.9	92.9±1.2	36.3±0.3	38.6±1.4
-	GCN _{knn} [22]	66.5±0.4	68.3±1.3	70.4±0.4	54.1±0.3	93.2±3.1	83.8±1.4	91.3±0.5	41.3±0.6
-	GAT _{knn} [40]	66.2±0.5	70.0±0.6	69.6±0.5	OOM	91.5±2.4	95.1±0.8	91.4±0.1	45.0±1.2
-	SAGE _{knn} [15]	66.1±0.7	68.0±1.6	68.7±0.2	55.2±0.4	87.4±0.8	93.7±0.3	91.6±0.7	45.4±0.4
X, Y	LDS [12]	71.5±0.8	71.5±1.1	OOM	OOM	97.3±0.4	94.4±1.9	92.5±0.7	46.4±1.6
X, Y, A _{knn}	GRCN [53]	69.6±0.2	70.4±0.3	70.6±0.1	OOM	96.6±0.4	95.4±0.6	92.8±0.2	41.8±0.2
X, Y, A _{knn}	Pro-GNN [20]	69.2±1.4	69.8±1.7	OOM	OOM	95.1±1.5	96.5±0.1	93.9±1.9	45.7±1.4
X, Y, A _{knn}	GEN [45]	69.1±0.7	70.7±1.1	70.7±0.9	OOM	96.9±1.0	<u>96.8±0.4</u>	94.1±0.4	47.1±0.3
X, Y	IDGL [7]	70.9±0.6	68.2±0.6	70.1±1.3	55.0±0.2	<u>98.1±1.1</u>	95.1±1.0	93.2±0.9	48.5±0.6
X, Y	SLAPS [11]	73.4±0.3	<u>72.6±0.6</u>	74.4±0.6	56.6±0.1	96.6±0.4	96.6±0.2	94.4±0.7	50.4±0.7
A _{knn}	GDC [23]	68.1±1.2	68.8±0.8	68.4±0.4	OOM	96.1±1.0	95.9±0.4	92.6±0.5	46.4±0.9
X	SLAPS-2s [11]	72.1±0.4	69.4±1.4	71.1±0.5	54.2±0.2	96.2±2.1	95.9±1.2	93.6±0.8	47.7±0.7
X	SUBLIME	<u>73.0±0.6</u>	73.1±0.3	<u>73.8±0.6</u>	<u>55.5±0.1</u>	98.2±1.6	97.2±0.2	<u>94.3±0.4</u>	<u>49.2±0.6</u>

Experiments

Table 2: Node classification accuracy (percentage with standard deviation) in structure refinement scenario.

Available Data for GSL	Method	Dataset			
		Cora	Citeseer	Pubmed	ogbn-arxiv
-	GCN	81.5	70.3	79.0	71.7±0.3
-	GAT	83.0±0.7	72.5±0.7	79.0±0.3	OOM
-	SAGE	77.4±1.0	67.0±1.0	76.6±0.8	71.5±0.3
X, Y, A	LDS	83.9±0.6	74.8±0.3	OOM	OOM
X, Y, A	GRCN	<u>84.0±0.2</u>	73.0±0.3	78.9±0.2	OOM
X, Y, A	Pro-GNN	82.1±0.4	71.3±0.4	OOM	OOM
X, Y, A	GEN	82.3±0.4	<u>73.5±1.5</u>	80.9±0.8	OOM
X, Y, A	IDGL	<u>84.0±0.5</u>	73.1±0.7	83.0±0.2	72.0±0.3
A	GDC	83.6±0.2	73.4±0.3	78.7±0.4	OOM
X, A	SUBLIME	84.2±0.5	<u>73.5±0.6</u>	<u>81.0±0.6</u>	<u>71.8±0.3</u>

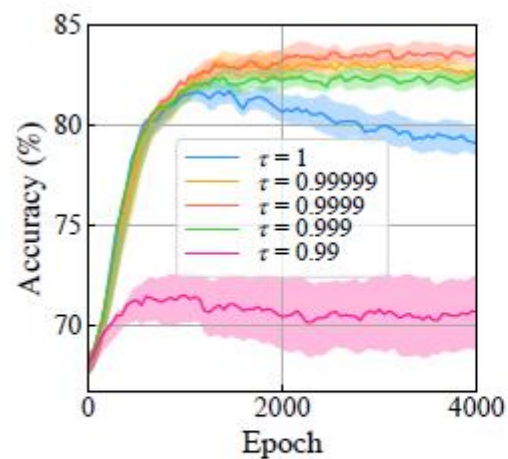
Table 3: Node clustering performance (4 metrics in percentage) in structure refinement scenario.

Method	Cora				Citeseer			
	C-ACC	NMI	F1	ARI	C-ACC	NMI	F1	ARI
K-means	50.0	31.7	37.6	23.9	54.4	31.2	41.3	28.5
SC	39.8	29.7	33.2	17.4	30.8	9.0	25.7	8.2
GE	30.1	5.9	23.0	4.6	29.3	5.7	21.3	4.3
DW	52.9	38.4	43.5	29.1	39.0	13.1	30.5	13.7
DNGR	41.9	31.8	34.0	14.2	32.6	18.0	30.0	4.3
M-NMF	42.3	25.6	32.0	16.1	33.6	9.9	25.5	7.0
RMSC	46.6	32.0	34.7	20.3	51.6	30.8	40.4	26.6
TADW	53.6	36.6	40.1	24.0	52.9	32.0	43.6	28.6
VGAE	59.2	40.8	45.6	34.7	39.2	16.3	27.8	10.1
ARGA	64.0	44.9	61.9	35.2	57.3	35.0	54.6	34.1
MGAE	68.1	48.9	53.1	56.5	66.9	<u>41.6</u>	52.6	<u>42.5</u>
AGC	68.9	<u>53.7</u>	<u>65.6</u>	44.8	67.0	41.1	62.5	41.5
DAEGC	<u>70.4</u>	52.8	68.2	49.6	<u>67.2</u>	39.7	63.6	41.0
SUBLIME	71.3	54.2	63.5	<u>50.3</u>	68.5	44.1	<u>63.2</u>	43.9

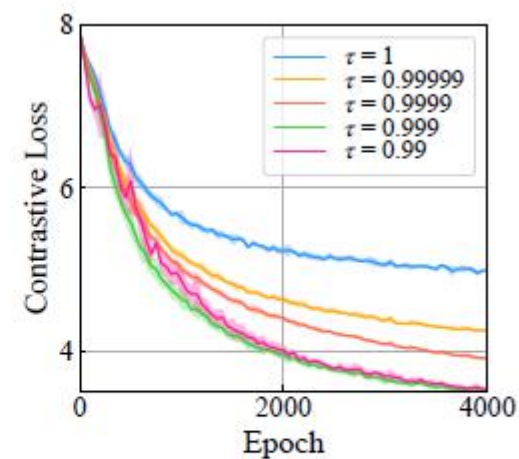
Experiments

Table 4: Test accuracy corresponding to different bootstrapping decay rate τ in structure refinement scenario.

Dataset	Bootstrapping decay rate τ				
	1	0.99999	0.9999	0.999	0.99
Cora	82.1	83.2	84.2	82.4	70.9
Citeseer	71.9	72.6	73.5	73.4	72.6
Pubmed	80.1	80.3	81.0	80.8	80.5



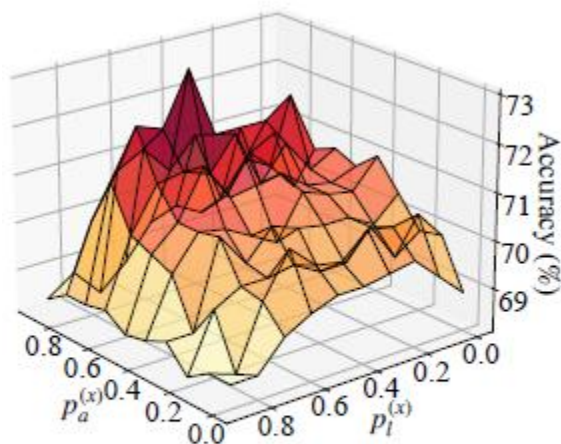
(a) Test accuracy w.r.t. epoch.



(b) Contrastive loss value w.r.t. epoch.

Figure 3: Curves of training process on Cora dataset.

Experiments



(a) Accuracy w.r.t. feature masking rates. (b) Accuracy w.r.t. number of neighbors.

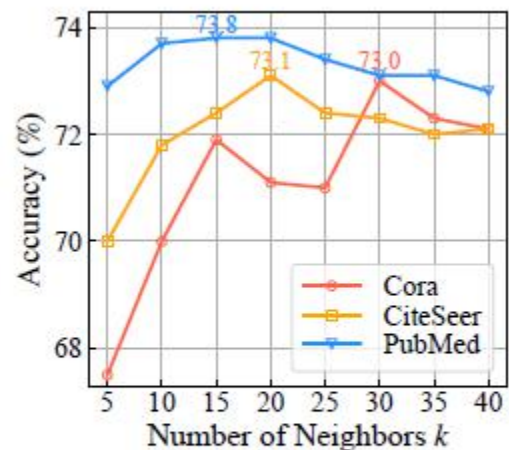
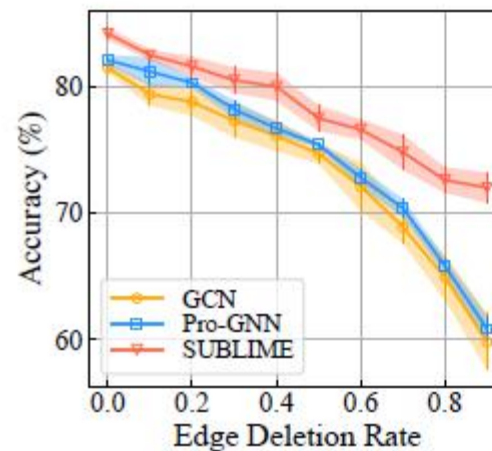
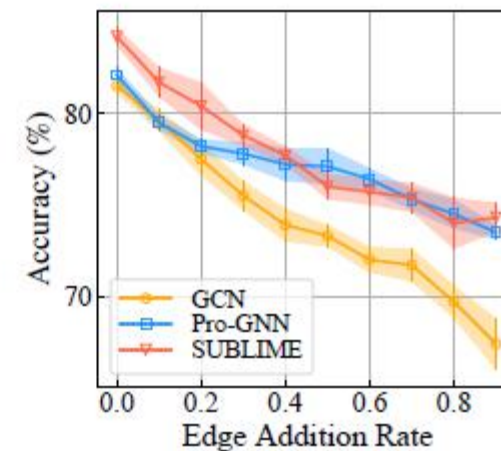


Figure 4: Sensitivity of hyper-parameters $p^{(x)}$ and k .



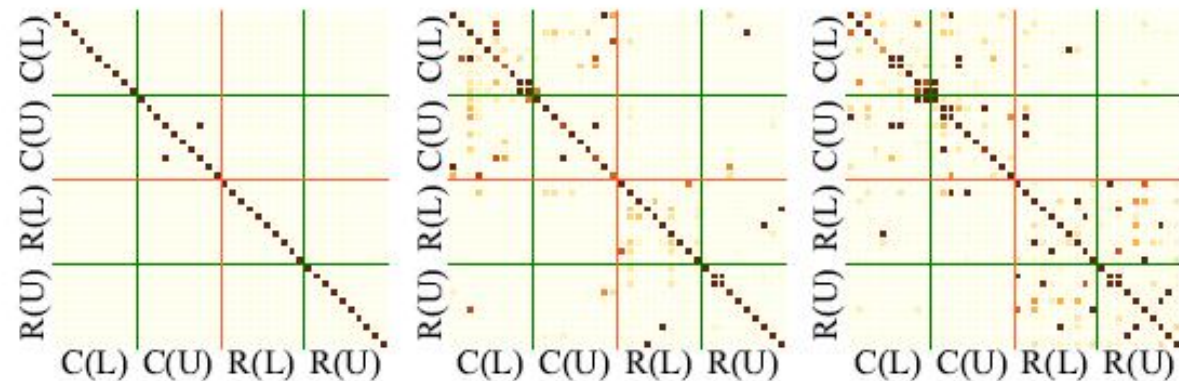
(a) Accuracy w.r.t. edge deletion rate.



(b) Accuracy w.r.t. edge addition rate.

Figure 5: Test accuracy in the scenarios where graph structures are perturbed by edge deletion or addition.

Experiments



(a) Original graph. (b) Graph learned by Pro-GNN. (c) Graph learned by SUBLIME.

Figure 6: Heatmaps of the subgraph adjacency matrices of (a) the original graph with self-loop, the graph learned by (b) Pro-GNN and (c) SUBLIME on Cora dataset. A block in darker color indicates a larger edge weight between two nodes.



Thank you!